Optimal Stator Design for Oxide Films Shearing Found by Physical Modelling

Agnieszka Dybalska, Dmitry G. Eskin and Jayesh B. Patel

Abstract A new technology suggests breaking oxide films into small fragments or particles to play the role of a grain refiner. A high-shear mixer (HSM) with a rotor-stator impeller can produce mechanical breakage. Physical modelling with powders demonstrates the defragmentation potency of HSM. Optimisation methods are considered and a new design of HSM is proposed according to the experimental findings. This design improves the uniformity of mixing in the pseudo-cavern volume and exhibits the dispersion efficiency better than the design previously used. The understanding and development of high shear technology for processing of liquid metals is of great interest to the industry.

Keywords Liquid metal · High shear · Rotor-stator · Pseudo-cavern Defragmentation · Stator design

Introduction

The necessity of the research focused on the oxides in the liquid metals, especially light ones as aluminium and magnesium, is caused by their harmful role of factor facilitative for the porosity and cracking of the cast material. The large oxide films and clusters in aluminium are usually distributed non-uniformly in the melt and have poor wettability [1–4]. Then again, wetted and dispersed oxides may act as good nucleating substrates for aluminium and magnesium [5–8]. Thus, mechanical breakage of clusters [9, 10] and dispersion thereof in the liquid metal can change the situation. The intensive melt shearing by special devices, for example, a rotor-stator impeller is believed to be a reason for the films breaking into small fragments or particles. The underlying mechanisms, which explain the observed reduction in grain size after melt shearing, were reported elsewhere [11–14].

A. Dybalska (✉) · D. G. Eskin · J. B. Patel
BCAST, Brunel University London, Uxbridge UB8 3PH, UK
e-mail: dybalska.ag@gmail.com

G. Lambotte et al. (eds.), *Materials Processing Fundamentals 2019*, The Minerals, Metals & Materials Series, https://doi.org/10.1007/978-3-030-05728-2_17

Materials and Methods

The mixer used was a Silverson L5M Laboratory Mixer. The motor has a power of 750 W, the impeller used has a diameter of about 25 mm. For the stators that were used, the rotational speed (N) of the HSM could be chosen for up to 9000 rpm. The rotor was inside the impeller, surrounded by the stator, which could be changed. The specification of the ordered stators is shown in the inset in Fig. 4. The first stator (RH, Fig. 4b), with round holes arranged in rows is designated to repeat a design that up to now had been used in liquid metal processing (prototype in Fig. 4a). The second stator (SqH) has a similar design, except for the shape of the holes, which are square (Fig. 4c). The last stator has other round holes arrangement (in cross lines) than used before (crossH, Fig. 4d). The holes have a specific size, 3 mm (diameter or height). More exact technical details could be found in [15] in the technical drawings.

In this choice of stator shape, we were able to easily compare the influence of the shape of the stator holes. The flow patterns have been observed in the water-model system. Water can mimic aluminium flow behaviour and is often used as a modelling material (i.e., Refs. 16, 17, 18, 19) because the essential properties of water at room temperature are similar to those of liquid aluminium and because both are Newtonian fluids. The investigation in the xz-plane was done by alumina powder pattern studies. PIV (particle image velocimetry) photographs were taken in the xy-plane to complete and confirm previous research results. On each occasion, the HSM was placed in a slightly off-centre position in the tank (sized 260 mm $\times$ 260 mm $\times$ 800 mm and a water level of 200 mm from the bottom) to avoid unnecessary surface vortexing in an unbaffled vessel [20].

Still photos and movies of the water were taken using a Fuji digital camera and a PIV system [21]. PIV relies on sequential images of visible features within the flow, which is not invasive for flow behaviour. To improve visibility fluid flow was seeded with particles that follow the fluid motion. Spherical particles, usually coated to reflect laser light were used to avoid alteration. In this research, we used the 8–12 μm hollow glass spheres [22]. A laser sheet in the region of interest illuminates the particles and the scattered light produces a tracer field for image capture [21]. To avoid the scattering of the light from the metal impeller, a laser light sheet was placed just in front of the head of the HSM. A schematic diagram of the system is shown in Fig. 1.

Intervals of 100 μs for recording the photographic sequences were chosen experimentally to achieve a reasonable quality of the pictures. For each experiment, those photographic sequences were taken at least 50 times when the laser beam was turned on using the high-speed camera. Using the Insight-6 software, the vector and velocity magnitude plots were drawn with the expected maximum error of around 0.1 pixels [23]. To confirm the results done by observing the powder pattern, we have to keep the height around 30 mm above the bottom [15] and that clearance results in a scattered flow from the bottom, but not from the walls.

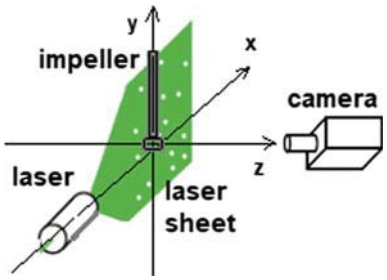

Fig. 1 Schematic diagram of the PIV system. The laser sheet illuminates the particles moving inside a glass tank (not shown in the diagram)

Results and Discussion

To improve the processing conditions we aim to find the optimal stator design and that is what this paper discusses. The main issue is the uniform dispersion of the sheared clusters as well as their effective fragmentation. Our consideration focused on the uniformity of the mixing inside the well-mixed region compared (the so-called pseudo-cavern [24, 25]), for each stator design. The different stator designs were checked by experimental shearing of alumina powder, which allows us to compare the fragmentation potency.

Commercial dispersion stators used for dispersion purposes have square holes [26]. The rotor-stator head used to improve the liquid metal quality is made from ceramic-like materials different from commercially used steel and each significant change will increase the costs. Because ceramic-like materials have high elastic modulus and hardness, preparing the square-shaped holes is much more difficult and expensive than for round-shaped holes. This is why a prototype head has simple rows of circular holes. The main question was how to improve this design to achieve the best results without the unnecessary increase in costs. To find an answer we have to compare the mixing efficiency and potency in the defragmentation of all the stators.

Mixing Uniformity

The first simple observations were made with alumina powder placed in the tank filled with water. During powder processing, the trace on the bottom reveals some uniformity different for different stators used (see Fig. 2). Analytical consideration lets us suppose that the strong jets localised in one direction can be the reason for that non-uniformity. To improve the uniformity of the mixing, the crossH design has been proposed. The idea is explained in Fig. 3.

In the case of the RH, the jets emerging from the stator openings are not distributed randomly around the head and there is a possibility that stagnation areas occur between them. To avoid this problem the proposed head has a cross-line arrangement of holes. Secondly, this change costs little as we only changed the placement of the

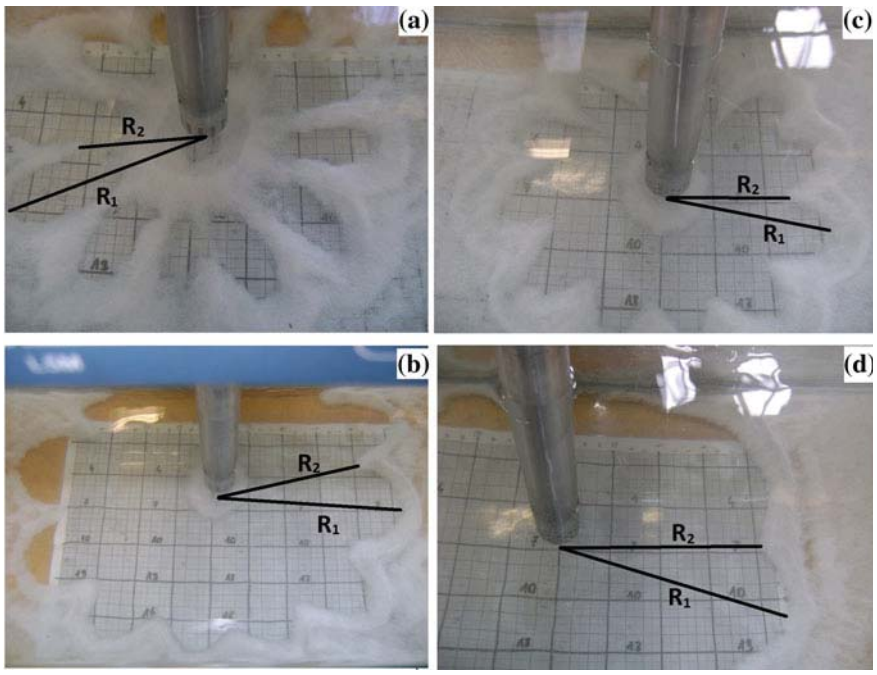

Fig. 2 The non-uniformity of mixing observed for RH and crossH stator. **a** RH, 3000 rpm, **b** RH, 5000 rpm, **c** crossH, 3000 rpm, **d** crossH, 5000 rpm

holes on the stator. To check how the proposed changes influence the uniformity of the mixed region we took the photographs of the created pattern after shearing the powder by both heads. The difference between the radii of the mixed region measured along the jets (R_1) and along the more stagnant zones (R_2) between them is taken as the non-uniformity coefficient $\Delta R = R_1 - R_2$ (see Fig. 2).

The measurements presented in Table 1 suggest that non-uniformity of the mixed region is smaller with the crossH design and it is comparable to the SqH head. The non-uniformity coefficient found for the RH stator is about 2–5 times larger than the one measured for the crossH. The low uniformity level observed has been seen not only for powder patterns, but it is also indicated by the PIV velocities pattern for this stator—the agitated region observed in the cross section is much smaller than for other stators, what can be associated with the presence of stagnant regions around this head. PIV photographs of the flow that will be discussed further (see Fig. 5).

An additional analysis, confirmed by the PIV observations, gives more specific information about that well-mixed region volume. In Fig. 6, the volume dependence on N for all is compared for each stator. The volume has been approximated as an ellipsoid and the size of the well-mixed region along x and y directions was established by physical modelling in water. The detailed procedure of volume calculations can be found elsewhere [15].

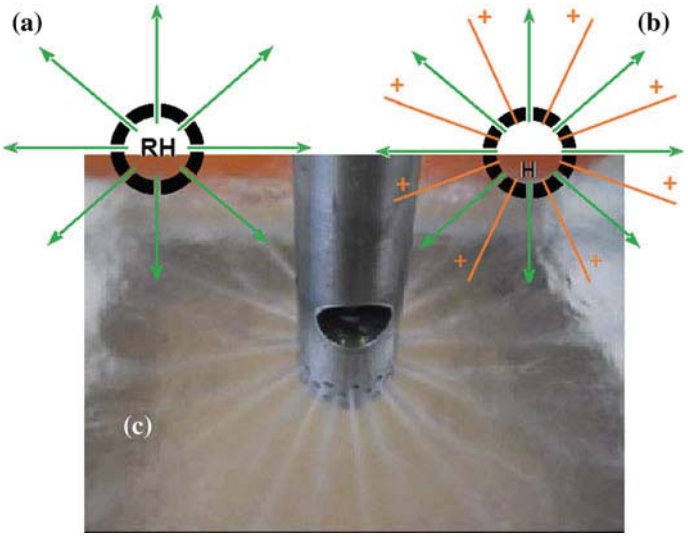

Fig. 3 **a** Schematic illustration of the jets' directions around the RH stator, **b** Schematic illustration of the jets' directions around the crossH stator, additional (+) positions of jets are the effect of the holes' rearrangement on the stator that improves uniformity. **c** Jets observed in 3D for crossH. To observe them only the bottom of the head was immersed in water. The sucking force brought a liquid to the head and spread it out as the jets travelled in the air

Table 1 The average non-uniformity coefficient ΔR measured experimentally from the traces of the well-mixed region on the bottom of the tank in water and alumina powder system

N	ΔR for RH (mm)	ΔR for crossH (mm)	ΔR for SqH (mm)
2000	10 ± 2	5 ± 1	10 ± 2
3000	10 ± 2	5 ± 1	5 ± 1
4000	10 ± 2	5 ± 1	0 ± 1
5000	10 ± 2	2 ± 1	0 ± 1
6000	5 ± 1	0 ± 1	0 ± 1

At least 10 coefficients for each stator design and specific N were measured

A predicted volume of the well-mixed region calculated for crossH is in the similar range as the one calculated for SqH and slightly smaller than the one observed for RH (Fig. 4). The prediction is based on jet length, and since the jets come from the holes arranged in the rows, they join causing a strong movement of the fluid which travels farther. It does not necessarily mean the full agitation of the fluid. In between these conjoined jets, there are stagnant zones. The strong jets have a longer travel distance, and calculations of the volume are based on maximal jet length. Therefore, the non-uniformity is not taken into account in Fig. 4. The mixed volume is also smaller when the holes are square-shaped than when they are round. The reason for this can be explained by the jets' impairment on the hole boundary. Round holes

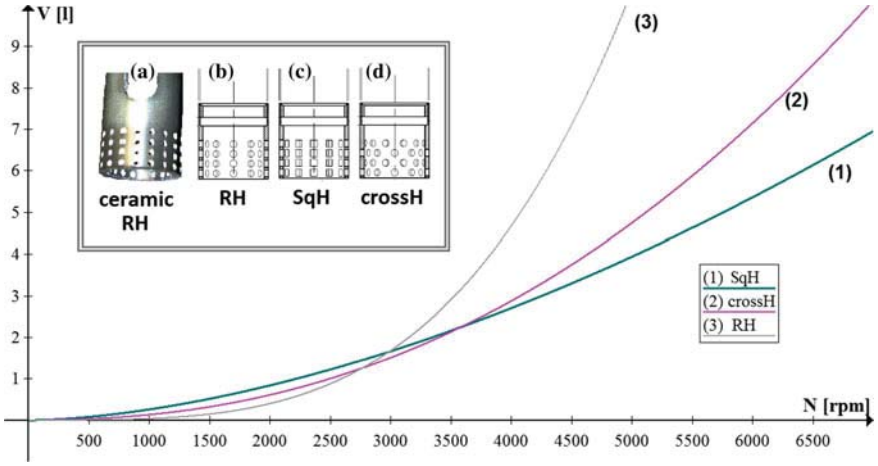

Fig. 4 Predicted volumes of the pseudo-cavern observed with different stators for a wide range of the N. In the inset: different shapes of stators, **a** prototype ceramic stator used to shear molten, **b** model of the ceramic stator, RH stator with round holes in the rows, **c** SqH stator with square-shaped holes, **d** crossH stator with proposed change of holes arrangement

do not disturb jets and allow them to move more freely than the square ones. The free jets tend to acquire a cylindrical shape, which is an effect of the surface tension holding droplets together. If no other forces are present, the free jet maintains its shape for a specific length and will be broken in droplets in the air [27, 28; after 29] or will change from the concentrated form of the jet into the turbulence of the fluid [30].

Before this happens, just after passing the hole, the contraction can be observed and the jet diameter will become smaller than the hole aperture [31]. Thus, the jet shape is always close to a cylinder. The square hole will change this natural shape by mechanical reflections of the fluid, which means that the "square jet" becomes less stable. This effect was illustrated and predicted by computer simulations. Isosurfaces of the velocity gradient tensor for circular and square jets show that the turbulence at the end of the jet occurs earlier in the case of the square jet [30]. Less stability of the jets is a simple reason for the observation presented in Fig. 4 and it explains why the mixed volume is bigger for RH since the expected jets are longer for the RH stator.

Since RH and SqH compared in Fig. 4 have the same design, except for the shape of the holes, in the chosen N, the moving rotor gives the same amount of energy into a fluid. As the mixed region seems to be smaller for the SqH, it means that part of the energy is used for a process other than mixing, or the agitation inside the pseudo-cavern is more intensive. To find an explanation for this difference in volumes we need to compare the flow around all the stators. The flow pattern observed with a PIV system is shown in Fig. 5.

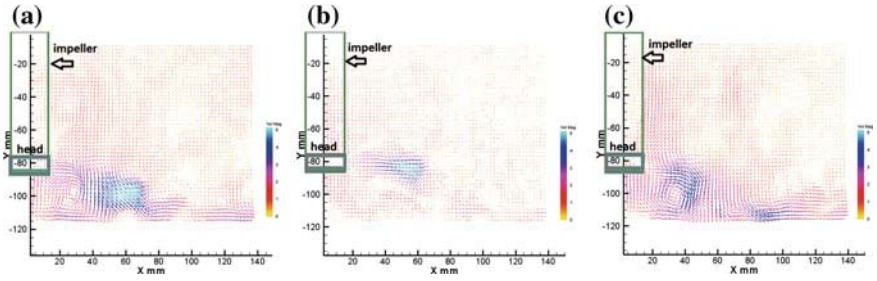

Fig. 5 **a** Flow around the SqH stator; **b** flow around the RH stator, **c** flow around the crossH stator. The head position is shown by the red rectangular, N = 7000 rpm. Velocities on the scale bars are given in m/s

The flow observed in the xy-plane was mainly recorded to confirm the size of the well-mixed region but recorded photographs offer complex information. In the pictures (Fig. 5), we can observe proof of the non-uniform agitation in (b) part of the figure. The flow is much weaker than that recorded with other stators. Surprisingly the jet does not start near the stator. Obviously, the laser beam plane reveals the stagnation zone in this area and part of the jet above point on the x-axis over 30 mm. For SqH and crossH, any of the recorded PIV photographs (taken in the range 2000–9000 rpm with a step of 1000 rpm) have not shown a similar flow pattern. In each case recorded for those stators, the flow pattern was more uniform as in cases (a) and (c). The RH recorded for the same range gives a "weak" pattern twice. Thus, it is a strong indication that sometimes the beam crosses the stagnation area around the RH head, which is consistent with the previous measurements of the non-uniformity coefficient. Similar observations can be found in the Mortensen's et al. research [32], around the used slotted head investigated by the PIV system. The slotted stator is slightly similar to the RH, but instead of the row of round holes, there is one slot.

PIV photographs [32] of the flow reveal a strong jet surrounded by a reverse fluid with much smaller velocities. Since their observation plane was perpendicular to what is shown in Fig. 4, we can complement our knowledge with these findings. According to the results published by Mortensen [32], we can expect strong jets to be accompanied by regions of stagnation or weaker reversed flow, which is the result of fluid inertia. It is not surprising that the RH stator with rows of round holes causes the same effect, since the jets from each hole can join to create a similar flow pattern as for the slotted head.

It should be reminded here that the round holes are the beginning of strong and concentrated jets, while the square-holes stator provides a more uniform mixing since the jets are not so well concentrated. The jets will not travel as far with round holes but the velocity pattern is more uniform because the energy is transferred by the turbulence on the end of the jet into the fluid surrounding the jet. The better agitation can be seen in Fig. 4 as the flow observed with an SqH stator is more agitated and the calculated mean velocities differ by as much as 28% for the case in Fig. 4. When the N increases, the difference increases too [15].

After PIV analyses, we can conclude that even if the volume calculated for RH is slightly bigger than for SqH, it is accompanied by the decrease in the uniformity and intensity of the agitation inside the well-mixed volume. The intensity of the agitation was previously checked for few Silverson stators by the computer simulation [33] and it was found that in the case of the square-hole head from the Silverson provider about 28% of the energy is dissipated in the jet region and in the rest of the tank. For disintegrating the head in a similar region, the amount of energy dissipated equals 43%. Thus, jet energy and tank agitation are on a higher level with wide round holes (8 mm diameter). In the case of narrower (1.6 mm wide slots with the length of 11 mm) and square-shaped holes (2.5 mm), about 18% more energy is dissipated in the rotor swept region and in the holes region than in the case of the disintegrating head. That means that more energy is used for the shearing process that occurs inside the head and in the holes region than in the case of the disintegrating head. The RH (Fig. 4b) has some similarities to the disintegrating head. The holes of the RH are smaller but the same round shape will be promoting the free jets emanating from the stator holes. Therefore, the jets will transfer more energy outside the head. If we compare only the well-mixed region (jets region at [33]), it can be seen that the agitation is slightly less for the disintegrating head. The non-uniform agitation of this region can give an explanation. Similar results are observed in our research for RH as the averaged velocities are smaller in this region than with the SqH stator [15].

The observations presented here are in good agreement with results of computer simulation done previously [33], since square holes, according to PIV results, are accompanied by a more uniform and concentrated flow inside the pseudo-cavern. Author of [33] also described that the energy dissipated around the square-holed head is more intensive inside the jet region than observed with other stators. Additionally, for square holes, only 1% of the energy is transferred to the rest of the tank, which indicates the intensification of the well-mixed volume (especially when compared to 20% of energy transferred by the disintegrating head).

The mixing efficiency of the crossH stator is better than that of the RH design. Using square holes will be even beneficial, but if that is non-economical, the RH stator should be replaced by the crossH design to improve mixing uniformity until the defragmentation potency is comparable, which is discussed in the next section.

Fragmentation Potency

The last presented set of experiments was prepared to check the potency of the defragmentation of all stators. To compare results, the powders were observed and the cross-sectional area of particles was measured. As an effect, we present the frequency distribution of particles area (FDPA) of alumina sheared by each stator. Figure 5 shows the results of the alumina shearing by the SqH compared to the results of shearing by the RH and proposed the crossH stator. Examples of the pictures taken by microscope for the epoxy-mounted powders are given in the inset.

The sheared powder was alumina, bonded with ion bonds into bigger granules. In the molten metal, oxides are present as films and clusters joined by van der Waals attractive forces. The van der Waals bond is the weakest of all bond types; the strength of the van der Waals force is between 0.01 and 0.1 eV per bond [34, 35] while aluminium oxide molecules are bonded by ionic bonds with a typical energy of about 8–10 eV [36], which means that in the experiments described here we are breaking bonds about 100–1000 times stronger than those expected to bond oxide films and agglomerates in the melt.

The agglomeration process is often described as a stochastic process [37] because it depends on local and temporary conditions; for example, the number of particles in agglomerates. May be we cannot predict the exact bonding forces, but we can refer to real shearing effects, which are documented by a grain size refinement [11–14]. This is indirect evidence that the shear applied by using a "round" head is enough to break oxide agglomerates and films. Men et al. [37] investigated the mechanisms of grain refinement by intensive melt shearing and found that it can effectively disperse MgO films into more individual particles using the RH head. The MgO particle density was three orders of magnitude higher than without shearing, as found by analysing the size distribution of the particles found by the pressurised filtration [37]. Thus, if the RH is proven to cause the oxide agglomerate defragmentation, other considered designs can be compared with this base-one. The alumina size reduction is stronger for powder processed by SqH and crossH stators in comparison to RH (see Fig. 6, inset) and both stators should be considered for liquid metal processing.

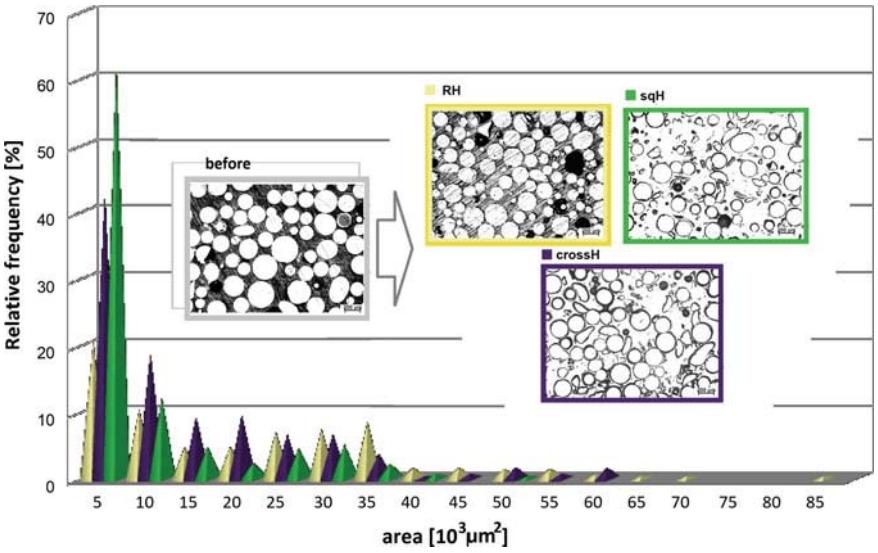

Fig. 6 The histogram of the FDPA for sheared alumina particles with different stators calculated from the powder pictures (an example is given in the insets)

The number of holes, time and mixing speed were the same for both experiments. Thus, we observe the only effect is the change in the shape of the holes. If we compare the percentage results (see Fig. 6) for SqH and RH, we can state, that for a square-holed head over 70% of the particles are in the range of 0–10,000 μm^2. For the round-holed head only 30% of the particles are in this range. It shows that square holes are really effective to shear used hard particles. However, if the costs of the square holes preparation are too high we can improve the effects of shearing by making other changes. The proposed change in holes arrangement (crossH, see Fig. 3) results in the change in local pressure inside the head. In the case of the RH, the pressure exerted on the stator walls by the fluid is stronger close to areas between the rows, where holes are not present. Inside the new head, we expect smaller differences between the local pressures as the area between the holes has a more uniform size. To check how this local change in pressure influences the shearing potency we can check the size of the processed alumina. If we take one more look at Fig. 6, we notice the particles broken by the crossH have mostly cross-sectional areas below or equal to 10,000 μm^2 and about 60% of them are in this range, 30% more than for RH. Obviously, the uniformity of the mixing inside the rotor-stator assembly does not decrease the fragmentation potency and even improves the shear process.

Concluding Remarks

The physical modelling proved that the HS processing of liquid metals is a potent method to achieve the defragmentation of agglomerates, as the defragmentation of the alumina occurs in all the experiments presented. The defragmentation efficiency is strongly influenced by the shape of the stator holes and the best results were obtained with square holes. However, the defragmentation potency of round holes for oxides present in the melt was proven experimentally.

The uniformity of the mixing inside the well-mixed region was checked for different mixing conditions and, according to the results, a new stator design was proposed for treating liquid aluminium. This design improves the uniformity of the mixing in the well-mixed volume and has higher dispersion efficiency than the design used up to now.

Acknowledgements Allocation of the equipment in the BCAST (Brunel University London) is highly appreciated. The first author is grateful for Ph.D. study funding from the Institute of Materials and Manufacturing, Brunel University London. The authors would also like to acknowledge Prof. Z. Fan, who initiated this research. The PIV measuring system was provided by the EPSRC Engineering Instrument Pool.

References

1. Green NR, Campbell J (1993) Statistical distributions of fracture strengths of cast A1-7Si-Mg alloy. Mater Sci Eng A 173:261–266
2. Mi J, Harding RA, Campbell J (2004) Effects of the entrained surface film on the reliability of castings. Metall Mater Trans A 35(9):2893–2902
3. Nyahumwa C et al (1998) Effect of mold-filling turbulence on fatigue properties of cast aluminum alloys. Paper presented at the 102nd Casting Congress, Atlanta, Georgia, 10–13 May 1998
4. Wang QG, Apelian D, Lados DA (2001) Fatigue behavior of A356-T6 aluminum cast alloys. Part I. Effect of casting defects. J Light Met 1(1):73–84
5. Fan Z (2011) Epitaxial nucleation and grain refinement. Paper presented at the John Hunt International Symposium, Uxbridge, London, 12–14 Dec 2011
6. Men H, Fan Z (2011) Effects of lattice mismatch on interfacial structures of liquid and solidified Al in contact with hetero-phase substrates: MD simulations. Paper presented at the ICASP–3, Rolduc Abbey, Aachen, The Netherlands, 7–10 June 2011
7. Tzamtzis S, Zhang H, Xia M, Babu NH, Fan Z (2011) Recycling of high grade die casting AM series magnesium scrap with the melt conditioned high pressure die casting (MC-HPDC) process. Mater Sci Eng A 528(6):2664–2669
8. Li HT et al (2011) Harnessing oxides in liquid metals and alloys. Paper presented at the John Hunt International Symposium, Uxbridge, London, 12–14 December 2011
9. Scamans G et al (2012) Melt conditioned casting of aluminum alloys. Paper presented at ICAA13, Pittsburgh, Pennsylvania, 3–7 June 2012
10. Li HT, Scamans G, Fan Z (2013) Refinement of the microstructure of an Al-Mg_2Si hypereutectic alloy by intensive melt shearing. Mater Sci Forum 765:97–101
11. Patel J et al (2013) Liquid metal engineering by application of intensive melt shearing. Paper presented at LMPC 2013, Austin, Texas, 22–25 Sept 2013
12. Zuo YB et al (2011) Grain refinement of DC cast magnesium alloys with intensive melt shearing. Paper presented at the ICASP–3, Rolduc Abbey, Aachen, The Netherlands, 7–10 June 2011
13. Li HT, Wang Y, Fan Z (2012) Mechanisms of enhanced heterogeneous nucleation during solidification in binary Al–Mg alloys. Acta Mater 60:1528–1537
14. Li HT, Xia M, Jarry P, Scamans G, Fan Z (2011) Grain refinement in a AlZnMgCuTi alloy by intensive melt shearing: A multi-step nucleation mechanism. J Cryst Growth 314(1):285–292
15. Dybalska A (2016) Understanding and development of high shear technology for liquid metals processing. PhD thesis, Brunel University
16. Gupta D, Lahiri AK (1996) A water model study of the flow asymmetry inside a continuous slab casting mold. Metall Mater Trans B 27(5):757–764
17. Xu D, Jones W, Kinzy W, Evans JW (1998) The use of particle image velocimetry in the physical modeling of flow in electromagnetic or direct-chill casting of aluminum: Part I. Development of the physical model. Metall MaterTrans B 29:1281–1288
18. Zhang L, Yang S, Cai K, Li J, Wan X, Thomas BG (2007) Investigation of fluid flow and steel cleanliness in the continuous casting strand. Metall Mater Trans B 38(1):63–83
19. Karcz J, Szoplik J (2004) An effect of the eccentric position of the propeller agitator on the mixing time. Chem Pap-Slovak Acad Sci 58(1):9–14
20. Tzanakis I, Lebon GSB, Eskin DG, Pericleous KA (2017) Characterizing the cavitation development and acoustic spectrum in various liquids. Ultrason Sonochem 34:651–662
21. Raffel M, Willert C, Wereley S, Kompenhans K (2007) Particle imaging velocimetry—a practical guide, 2nd edn. Springer, Berlin
22. Adrian RJ, Westerweel J (2011) Particle image velocimetry. Cambridge University Press, Cambridge
23. Huang H, Dabiri D, Gharib M (1997) On errors of digital particle image velocimetry. MST 8(12):1427–1440
24. Doucet L, Ascanio G, Tanguy PA (2005) Hydrodynamics characterization of rotor-stator mixer with viscous fluids. Chem Eng Res Des 83(10):1186–1195

25. Barailler F, Heniche M, Tanguy PA (2006) CFD analysis of a rotor-stator mixer with viscous fluids. Chem Eng Sci 61(9):2888–2894
26. Apparatus and method for high-shear mixing. US. Patent Application, US20160271575A1. 22 Sept 2016
27. Rayleigh JWS (1891) Some applications of photography. Nature 44:249–254
28. Nollet, JA (1749) Recherches sur les causes particulieres des phénoménes électriques, et sur les effets nuisibles ou avantageux qu'on peut en attendre. A Paris: chez les Freres Guerin, Paris
29. Eggers J, Villermaux E (2008) Physics of liquid jets. Rep Prog Phys 71(3):036601
30. Gohil TB, Saha AK, Muralidhar K (2010) Control of flow in forced jets: a comparison of round and square cross sections. J Vis 13:141–149
31. Brodkey RS, Hershey HC (2003) Transport phenomena: a unified approach. Brodkey Publishing, Columbus, Ohio
32. Mortensen HH, Calabrese RV, Innings F, Rosendahl L (2011) Characteristics of batch rotor–stator mixer performance elucidated by shaft torque and angle resolved PIV measurements. Can J Chem Eng 89(5):1076–1095
33. Utomo AD (2009) Flow patterns and energy dissipation rates in batch rotor-stator mixers. PhD thesis, University of Birmingham
34. Roesler J, Harders H, Baeker M (2007) Mechanical behaviour of engineering materials. Springer, Berlin
35. Smirnov BM (1992) Cluster Ions and van der Waals Molecules. CRC Press, Boca Raton
36. Il'inskii YA, Keldysh LV (2013) Electromagnetic response of material media. Springer, Berlin
37. Men H, Jiang B, Fan Z (2010) Mechanisms of grain refinement by intensive shearing of AZ91 alloy melt. Acta Mater 58(18):6526–6534